

Viscosity of fused silica and thermal noise from the standard linear solid model

N. M. Kondratiev

Russian Quantum Center, Skolkovo 143025, Russia

M. L. Gorodetsky*

Russian Quantum Center, Skolkovo 143025, Russia and Faculty of Physics,

M. V. Lomonosov Moscow State University, 119991 Moscow, Russia

(Received 18 September 2016; published 27 October 2016)

The fluctuation-dissipation theorem states that each source of dissipation yields corresponding fluctuations. The most obvious source of dissipation in liquids is viscosity—internal friction between layers of matter. However, this property also exists in solid materials in a glass state, i.e., an amorphous substance that cannot become a crystal due to high viscosity. Fused silica is a low-loss glass material used in many interferometric applications demanding high stability, such as Fabry-Perot etalons and gravitational-wave detector mirrors and suspensions. Very high viscosity (from 10^{17} to 10^{40} Pa s in the literature) can be the source of additional noise and can influence the performance of such devices. We show that fused silica may be described with the standard linear solid model of viscoelasticity and present a method to estimate this type of noise.

DOI: [10.1103/PhysRevD.94.081102](https://doi.org/10.1103/PhysRevD.94.081102)

I. INTRODUCTION

For modern high-precision measurements any source of noise can be critical. The LIGO project [1] that resulted in the first direct observation of gravitational waves [2] has to account for many fundamental sources of fluctuations. The Brownian noise coming from chaotic thermal motion of particles is one of the enemies. Thermal noise in coatings, substrates, and suspensions of the interferometer's mirrors results in fluctuations of their surfaces which add phase noise to the signal [3,4]. A lot of other processes can degrade the sensitivity of the device [5,6].

The common way to calculate thermal noises is the fluctuation-dissipation theorem. It states that any dissipation in a system results in added fluctuations. The theory gives the spectral density of surface fluctuations in mirrors of the LIGO antennae in the form [3]

$$S(\omega) = \frac{4k_B T}{\omega} \text{Im}[\alpha_s + \alpha_j^c + \alpha_j^s], \quad (1.1)$$

where ω is the frequency, k_B is Boltzmann's constant, T is the temperature, α_s is the dynamic permittivity of the substrate, and α_j^c and α_j^s are the coating and coating-induced substrate dynamic permittivities. In Refs. [3,7,8] the values of these parameters were found to be

$$\alpha_s = \frac{1}{\sqrt{\pi w}} \frac{1 - \nu_s^2}{Y_s}, \quad (1.2)$$

$$\alpha_j^c = \sum_j \frac{\beta_j d_j}{\pi w^2} \frac{(1 + \nu_j)(1 - 2\nu_j)}{Y_j(1 - \nu_j)}, \quad (1.3)$$

$$\alpha_j^s = \sum_j \frac{d_j}{\pi w^2} \frac{Y_j}{1 - \nu_j^2} \frac{(1 + \nu_s)^2 (1 - 2\nu_s)^2}{Y_s^2}, \quad (1.4)$$

where w is the Gaussian beam radius on the mirror, Y_s and ν_s are Young's modulus and the Poisson coefficient of the substrate, Y_j and ν_j are the parameters of the j th coating layer, and d_j and β_j are the thickness and interference coefficient of the j th coating layer. The dissipation is then introduced empirically in the form of the loss angle $Y \rightarrow Y(1 - i\phi)$.

There are several models that try to describe this loss angle theoretically [9,10] and phenomenologically [11]. Viscosity is one of the sources of dissipation. In the following section we show that viscosity can be introduced into the equations in the same way, providing a new type of noise.

II. MODEL OF VISCOSITY

In hydrodynamics the viscosity can be introduced into the Navier-Stokes equation through the viscose stress tensor σ_{ik}^v :

$$\sigma_{ik}^v = \eta \left[\frac{\partial v_i}{\partial x_k} + \frac{\partial v_k}{\partial x_i} - \frac{2}{3} \delta_{ik} \frac{\partial v_l}{\partial x_l} \right] + \zeta \delta_{ik} \frac{\partial v_l}{\partial x_l}, \quad (2.1)$$

where η is the shear viscosity, ζ is the volume viscosity, and \vec{v} is the velocity of the particles. Combined with the tensor Hooke's law it gives the Kelvin-Voigt model for viscoelastic materials, which works well for modeling creep in solid materials [12]. This model was also successfully used to explain experimental data in Ref. [13]. However, this model does not give correct results for ultrasonic losses in our case of the high-viscosity limit, as in the spectral

*mg@rqc.ru

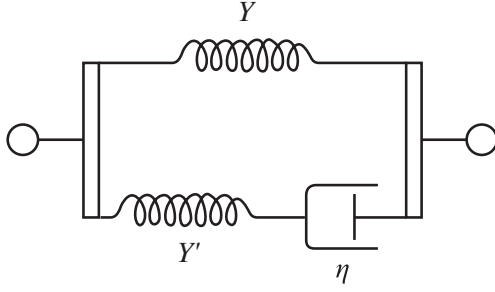


FIG. 1. “Elementary cell” of the SLS model.

representation it corresponds to a complex substitution of the shear and bulk moduli,

$$K \rightarrow K + i\omega\zeta, \quad (2.2)$$

$$G \rightarrow G + i\omega\eta. \quad (2.3)$$

It can be shown that this results in unrealistically high noise and even leads to the wrong dispersion relation for sound waves. There is another viscosity model, called the Maxwell model, which is usually used for glasses [14]. However, this model does not lead to the exponential matter flow rate measured in Ref. [15] and allows infinite motion that was not observed in experiment [16]. That is why we use the more general standard linear solid (SLS) model for viscoelastic materials [17].

The SLS model can be illustrated with the spring diagram, shown in Fig. 1. This “elementary cell” consists of a first (static or long-term) spring Y with shear and bulk moduli G and K , a second (dynamic) spring Y' with parameters G' and K' , and a dashpot with shear and bulk (volumetric) viscosity η and ζ . The first spring governs the static behavior of the system, while the higher-frequency motion uses both. Here we should note, however, that for ultra high viscosities of glasses all “static” load experiments are too fast for the second spring to relax (unless they are made on a time scale of years). In this way, both in measurements of the speed of sound and in static load experiments only the sum of the above introduced moduli is observed. This can also be shown directly using the model master equations (2.4), with the viscosities tending to infinity.

The master equation for the tensor stress-strain relationship in the standard linear solid model is

$$\begin{aligned} & \left(1 + \frac{G}{G'}\right) \dot{\varepsilon} + \frac{1}{3} \left(\frac{K}{K'} - \frac{G}{G'}\right) \text{tr}(\dot{\varepsilon}) + \frac{G}{\eta} \varepsilon + \frac{1}{3} \left(\frac{K}{\zeta} - \frac{G}{\eta}\right) \text{tr}(\varepsilon) \\ &= \frac{\dot{\sigma}}{2G'} + \frac{1}{3} \left(\frac{1}{3K'} - \frac{1}{2G'}\right) \text{tr}(\dot{\sigma}) + \frac{\sigma}{2\eta} + \frac{1}{3} \left(\frac{1}{3\zeta} - \frac{1}{2\eta}\right) \text{tr}(\sigma), \end{aligned} \quad (2.4)$$

where indices i and j in the stress and strain tensors notation σ and ε together with delta functions δ_{ij} in front of

the trace operators are omitted for simplicity. When the dynamic moduli $G', K' \rightarrow \infty$, we arrive at the Kelvin-Voigt model. When $K, G \rightarrow 0$ (long-term spring removed), we arrive at the Maxwell model. Finally, in the high-viscosity limit ($\eta, \zeta \rightarrow \infty$) the problem reduces to a general static problem with “quasistatic” moduli $G_0 = G + G'$ and $K_0 = K + K'$ that describe both high-frequency experiments and static load experiments held at time scales less than several years.

Taking the spectral representation of Eq. (2.4), we can get the following complex substitution for the shear and bulk moduli with which we can introduce viscous losses:

$$K \rightarrow K + \frac{i\omega\zeta K'}{K' + i\omega\zeta}, \quad (2.5)$$

$$G \rightarrow G + \frac{i\omega\eta G'}{G' + i\omega\eta}. \quad (2.6)$$

Unfortunately, the parameters of the model G', K', G , and K as well as the viscous parameters η, ζ at room temperatures are difficult to measure.

A. Standard linear solid parameters

To estimate the SLS parameters of fused silica a series of recent results [13,15,16] may be used. In those works a flow of fused silica plates under their own weight was studied over decades. We propose to reconsider these results in view of SLS model.

Assuming that the time dependence of the fields can be separated from the coordinate part so that $\hat{\varepsilon}(\vec{r}, t) = \hat{\varepsilon}(\vec{r})T(t)$ and $\hat{\sigma}(\vec{r}, t) = \hat{\sigma}(\vec{r})T_s(t)$, and using Eq. (2.4), we obtain

$$\frac{\sigma_{\mu>3}(\vec{r})}{\varepsilon_{\mu>3}(\vec{r})} = \frac{(1 + G/G')\dot{T} + GT/\eta}{\dot{T}_s/(2G') + T_s/(2\eta)} = C_G, \quad (2.7)$$

$$\frac{\text{tr}(\sigma(\vec{r}))}{\text{tr}(\varepsilon(\vec{r}))} = \frac{(1 + K/K')\dot{T} + KT/\zeta}{\dot{T}_s/(3K') + T_s/(3\zeta)} = C_K, \quad (2.8)$$

where $\mu > 3$ means nondiagonal terms (Voigt notation). The direct expressions for the stress tensor diagonal can also be obtained:

$$\frac{\sigma_{\mu\leq 3}(\vec{r})}{\varepsilon_{\mu\leq 3}(\vec{r})} = C_G + \frac{1}{3}(C_K - C_G) \frac{\text{tr}(\varepsilon(\vec{r}))}{\varepsilon_{\mu\leq 3}(\vec{r})}. \quad (2.9)$$

The form of the relations (2.7)–(2.9) suggests that there are probably two different oscillatory behaviors (e.g., time dependences) for diagonal (related to volumetric) and nondiagonal (related to shear motion) terms of the tensors. In this way the displacement vector may be decomposed into two parts as $\vec{u}(\vec{r}, t) = \vec{u}_K(\vec{r})T_K(t) + \vec{u}_G(\vec{r})T_G(t)$. So for the stress tensor we also can write $\hat{\sigma}(\vec{r}, t) = \hat{\sigma}_K(\vec{u}_K)T_{s_K}(t) + \hat{\sigma}_G(\vec{u}_G)T_{s_G}(t)$. Note that σ_G and σ_K act like linear differential operators.

The equation of elastic motion can be written as follows [18]:

$$\rho \ddot{\mathbf{u}} = -\rho \mathbf{g} + \text{div } \hat{\sigma}, \quad (2.10)$$

where ρ is the density, \mathbf{g} is the gravitational acceleration, and $\text{div } \hat{\sigma} = \frac{\partial \sigma_{ik}}{\partial x_k}$ in Cartesian coordinates. Substituting the above suggested decomposition into the homogeneous equations, we can see that due to linearity we can treat the equations for \vec{u}_K and \vec{u}_G separately. Furthermore, the equations are of the same form with respect to the partial index (K or G). The displacements should be matched to satisfy the boundary conditions. The solution can be introduced in the form of the sum of a particular solution of the full equation and a combination of solutions of the homogeneous equations. Nontrivial homogeneous equations of motion for cylindrical symmetry ($u_\varphi = 0$ and $\frac{\partial}{\partial \varphi} = 0$), omitting the part index, can be written as follows:

$$\rho \ddot{T} u_r = T_s \left(\frac{1}{r} \frac{\partial}{\partial r} (r \sigma_r) + \frac{\partial}{\partial z} \sigma_5 \right), \quad (2.11)$$

$$\rho \ddot{T} u_z = T_s \left(\frac{1}{r} \frac{\partial}{\partial r} (r \sigma_5) + \frac{\partial}{\partial z} \sigma_z \right). \quad (2.12)$$

Now by dividing the equations by T_s we collect all time-dependent variables on the right and coordinate-dependent variables on the left, thus performing coordinate separation. So we get $\ddot{T}/T_s = k^2$, where k^2 is the separation parameter in units of $1/(\text{Pa}^{1/2} \text{ s})$. This constant enumerates the solutions of the homogeneous equation and is to be summed over in an attempt to satisfy the boundary conditions. It is shown further that this value is not needed for the determination of the time constant. Combining this result with Eqs. (2.7) and (II.8), we find the temporal parts of the equations in the form

$$-k^2 \left((1 + G/G') \dot{T} + \frac{G}{\eta} T \right) = \frac{1}{2G'} \ddot{T} + \frac{1}{2\eta} \dot{T}. \quad (2.13)$$

The corresponding equation and solution for the volumetric part is obtained by changing $G \rightarrow K$, $\eta \rightarrow \zeta$, and $2 \rightarrow 3$. This equation for the high-viscosity approximation provides three time constants:

$$\gamma_0 = -\frac{GG'}{\eta(G + G')}, \quad (2.14)$$

$$\gamma_{\pm} = -\frac{G^2}{2\eta(G + G')} \pm ik\sqrt{G + G'}. \quad (2.15)$$

This results in a solution in the form of damped ($e^{\text{Re}\gamma_{\pm}t}$) oscillations with frequencies $\text{Im}\gamma_{\pm}$, near momentary equilibrium, exponentially ($e^{\gamma_0 t}$) approaching the final stationary displacement U_0 . Note that γ_0 do not depend on k meaning that it is the same for each solution of the coordinate part. This allow us to factorize the overall exponential decay tendency

from the sum of the solutions. In this way we obtain the exponential tendency function $U_0(1 - \exp(\gamma_0(t - t_0)))$ used in Ref. [15] to approximate the experimental data. Although it can be shown numerically that there is more energy in the volume part of the deformations, we assume that this exponential damping is related mostly to the shear process. The observable is the z displacement in the mirror's center which can be estimated as $\int_{\text{thickness}} \varepsilon_{zz} dz + \int_{\text{radius}} \varepsilon_{rz} dr$, and thus the shear part scales with the disc radius and prevails.

The parameters U_0 and γ_0^{-1} of the exponential approximation are badly determined (40% and 111% of the relative variance for 95% confidence). So we use estimations obtained for the last two plates [13]. It was shown that their relaxation has already finished (a year shift was less than the accuracy limit of 0.5 nm), allowing the authors to extract the parameters with 10% accuracy.

We can get an estimate for U_0 from the stationary consideration that obviously coincides with the common one [19,20]:

$$U_0 = \frac{g\rho R^2}{16Yh^2} (3(5R^2 + 4h^2) - 4(3R^2 - h^2)\nu - 3R^2\nu^2), \quad (2.16)$$

where $Y = \frac{9KG}{3K+G}$ is the Young modulus, $\nu = \frac{3K-2G}{2(3K+G)}$ is the Poisson ratio, R is the plate radius, h is its thickness, and ρ is its density. To complete the system of equations we use expressions for the longitudinal and transversal speeds of sound, modified according to the SLS model (2.5)–(II.6) in the high-frequency and -viscosity limit:

$$v_l^2 \approx \frac{3(K + K') + 4(G + G')}{3\rho}, \quad (2.17)$$

$$v_t^2 \approx \frac{G + G'}{\rho}. \quad (2.18)$$

In addition, we make the assumption that the Poisson ratio for the static parameters should be of the same order as that for the quasistatic one. Being small, this should be suitable for our estimations.

The results are summarized in Table I. The estimated viscosity is 10 times higher than that obtained in the original paper [13]. Nevertheless, it is still much less than the extrapolation values following from the high-temperature measurements.

TABLE I. Material parameters obtained from the literature and estimated.

Used	values	Estimated	values
U_0	35 nm	K	8.7 GPa
ν_0	0.17	G	7.3 GPa
c_t	3764 m/s	G'	23.8 GPa
γ_0^{-1}	12 years	η	$2.1 \times 10^{18} \text{ Pa} \cdot \text{s}$

N. M. KONDRATIEV and M. L. GORODETSKY

TABLE II. Substrate (*s*), high-refractive (*h*), and low refractive (*l*) layer parameters used for the calculation. The other constants are $\lambda = 1.064$ mkm, $w = 0.06$ m, and $T = 290$ K.

Layer	Y GPa	ν	n	ϕ
<i>s</i>	72	0.17	1.45	$7.6 \times 10^{-12} f^{0.77}$
<i>l</i>	72	0.17	1.45	0.4×10^{-4}
<i>h</i>	140	0.23	2.06	2.3×10^{-4}

III. VISCOSITY NOISE

We can now use the permittivities (1.2)–(1.4) with the substitution (2.5)–(2.6) to calculate the noises:

$$S_s = \frac{4k_B T}{\omega^2} \frac{1}{4\sqrt{\pi}w(v_l^2 - v_t^2)v_l^4 \rho^2} \times \left(v_l^4 \frac{K'^2}{\zeta} + (3v_l^4 - 6v_l^2 v_t^2 + 4v_t^4) \frac{G'^2}{3\eta} \right), \quad (3.1)$$

$$S_j^c = \frac{4k_B T}{\omega^2} \sum_j \frac{|\beta_j|^2 d_j}{\pi w^2} \frac{1}{v_l^4 \rho_j^2} \left(\frac{K_j'^2}{\zeta_j} + \frac{4G_j'^2}{3\eta_j} \right), \quad (3.2)$$

$$S_j^s = \frac{4k_B T}{\omega^2} \sum_j \frac{d_j}{\pi w^2} \frac{1}{(v_l^2 - v_t^2)^2 v_l^4 \rho^2} \times \left(2v_l^2 v_t^2 \frac{\rho_j (v_l^2 - v_t^2)}{\rho (v_l^2 - v_t^2)} \left(\frac{K'^2}{\zeta} + \frac{G'^2}{3\eta} \right) - \left(v_t^4 \frac{K_j'^2}{\zeta_j} + (3v_l^4 - 6v_l^2 v_t^2 + 4v_t^4) \frac{G_j'^2}{3\eta_j} \right) \right). \quad (3.3)$$

Here, v_l^2 and v_t^2 are longitude and transverse wave velocities of the substrate and *j*th layer, G' and K' are the short-time shear and bulk moduli of the substrate and *j*th layer, η and ζ are the shear and bulk viscosity of the

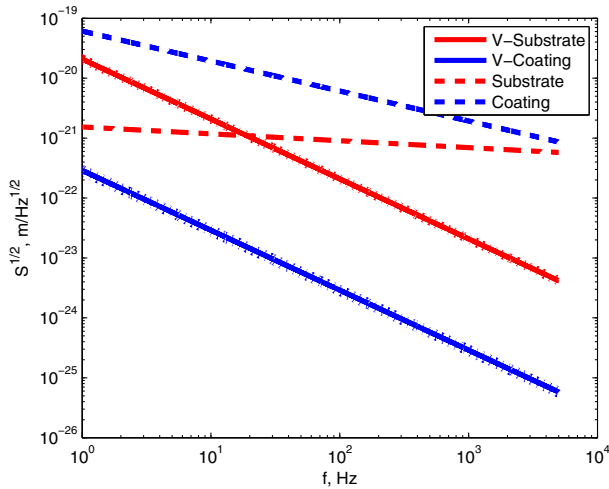


FIG. 2. Brownian noises from the substrate and coating (dashed lines) for the parameters from Table II according to Ref. [21] with viscosity noises (solid lines). The error estimation is 15% (dots).

PHYSICAL REVIEW D **94**, 081102(R) (2016)

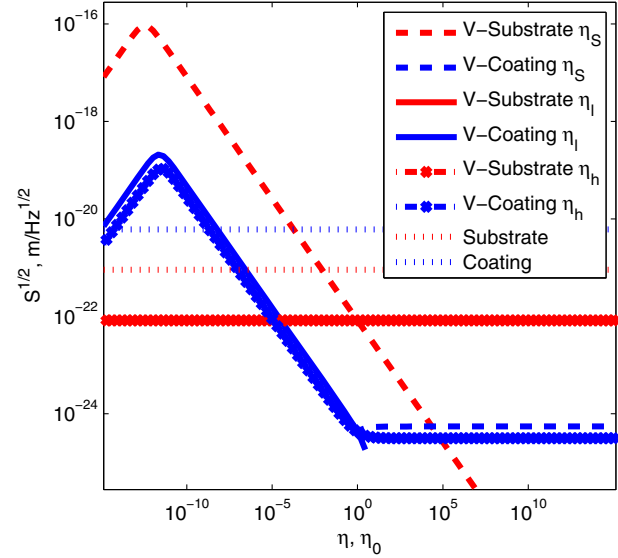


FIG. 3. Brownian and viscosity noises at 100 Hz depending on the viscosity of the substrate η_s , silica layer η_l , or tantala layer η_h in units of $\eta_0 = 2.1 \times 10^{18}$ Pa · s. The rest of the viscosities were taken equal to η_0 for each curve.

substrate and *j*th layer, and ρ represents the materials' densities.

We use the mirror parameters from Ref. [21], given in Table II. Here “l” stands for low-refraction material (silica), “h” stands for high-refraction material (tantala), and “s” stands for the substrate (high-quality silica). Y and ν are the Young modulus and Poisson ratio of the layers (used to estimate Brownian noises), n represents the refraction indices, ϕ represents the loss angles, λ is the laser wavelength, w is the laser beam spot radius (e^{-2} power), and T is the temperature.

The numerical estimates of the silica part together with the standard Brownian noise are shown in Fig. 2. The coating part appears to be several orders lower than the viscosity substrate noise due to its small thickness. It can be neglected until tantala has a viscosity at least 5 orders smaller than that of silica (see Fig. 3).

IV. CONCLUSION

The viscosity of fused silica can be the source of additional noise in LIGO antennae exceeding the substrate Brownian noise at frequencies below 19 Hz. However, if we use the viscosity value as calculated in Ref. [16] this point moves close to 100 Hz—the maximum of LIGO sensitivity. Furthermore, the whole volumetric part of the noise is unknown due to the absence of appropriate material parameters data.

Another uncertainty is attributed to viscosity in the mirror's coating which is totally unknown. Remembering that regular mechanical coating losses are 3 orders of magnitude higher than in bulk material (making coating

Brownian noise the limiting factor of the LIGO detector), viscosity in stressed coating may suggest surprises. Note that the lower the viscosity, the higher the noise. We also note that temperature reduction may be an efficient way to reduce the viscosity noise by increasing the viscosity itself. Nevertheless, the coating Brownian noise still remains the limiting factor for LIGO interferometers for now.

We also conclude that fused silica can be described by the Maxwell model of viscosity for times smaller than

12 years from the start of relaxation, while the SLS model should be used otherwise.

ACKNOWLEDGMENTS

The authors acknowledge support from the Russian Foundation for Basic Research (Grant No. 14-02-00399A) and National Science Foundation (Grant No. PHY-1305863).

-
- [1] B. P. Abbott *et al.* (LIGO Scientific and Virgo Collaborations), *Rep. Prog. Phys.* **72**, 076901 (2009).
 - [2] B. P. Abbott *et al.* (LIGO Scientific and Virgo Collaborations), *Phys. Rev. Lett.* **116**, 241102 (2016).
 - [3] G. M. Harry, A. M. Gretarsson, P. R. Saulson, S. E. Kittelberger, S. D. Penn, W. J. Startin, S. Rowan, M. M. Fejer, D. R. M. Crooks, G. Cagnoli, J. Hough, and N. Nakagawa, *Classical Quantum Gravity* **19**, 897 (2002).
 - [4] G. M. Harry, H. Armandula, E. Black, D. R. M. Crooks, G. Cagnoli, J. Hough, P. Murray, S. Reid, S. Rowan, P. Sneddon, M. M. Fejer, R. Route, and S. D. Penn, *Appl. Opt.* **45**, 1569 (2006).
 - [5] M. L. Gorodetsky, *Phys. Lett. A* **372**, 6813 (2008).
 - [6] M. Evans, S. Ballmer, M. Fejer, P. Fritschel, G. Harry, and G. Ogin, *Phys. Rev. D* **78**, 102003 (2008).
 - [7] A. Gurkovsky and S. Vyatchanin, *Phys. Lett. A* **374**, 3267 (2010).
 - [8] N. M. Kondratiev, A. G. Gurkovsky, and M. L. Gorodetsky, *Phys. Rev. D* **84**, 022001 (2011).
 - [9] R. Vacher, E. Courtens, and M. Foret, *Phys. Rev. B* **72**, 214205 (2005).
 - [10] A. E. Duwel, J. Lozow, C. J. Fisher, T. Phillips, R. H. Olsson, and M. Weinberg, *Proc. SPIE Int. Soc. Opt. Eng.* **8031**, 80311C (2011).
 - [11] S. D. Penn, A. Ageev, D. Busby, G. M. Harry, A. M. Gretarsson, K. Numata, and P. Willems, *Phys. Lett. A* **352**, 3 (2006).
 - [12] R. Tanner, *Engineering Rheology* (Oxford University, New York, 2000).
 - [13] M. Vannoni, A. Sordini, and G. Molesini, *Eur. Phys. J. E* **34**, 92 (2011).
 - [14] F. Richter, Ph.D. thesis, Technische Universitat Berlin, 2006.
 - [15] M. Vannoni, A. Sordini, and G. Molesini, *Opt. Express* **18**, 5114 (2010).
 - [16] M. Vannoni, A. Sordini, and G. Molesini, *Proc. SPIE Int. Soc. Opt. Eng.* **8169**, 816906 (2011).
 - [17] Y. de Haan and G. Sluimer, *Heron* **46**, 49 (2001).
 - [18] L. Landau, L. Pitaevskii, A. Kosevich, and E. Livshitz, *Theory of Elasticity* (Elsevier, New York, 2012).
 - [19] W. Emerson, *J. Res. Bur. Stand.* **49**, 241 (1952).
 - [20] S. Timoshenko and S. Woinowsky-Krieger, *Theory of Plates and Shells* (McGraw-Hill, New York, 1959).
 - [21] LIGO Scientific Collaboration, Gravitational wave interferometer noise calculator (GWINC), <https://awiki.ligo-wa.caltech.edu/aLIGO/GWINC>.